Hindawi
Advances in Civil Engineering
Volume 2018, Article ID 8985973, 9 pages
https://doi.org/10.1155/2018/8985973

Research Article

Effects of Cyclic Loading on the Mechanical Properties of Mature Bedding Shale

Yintong Guo, Chunhe Yang, Lei Wang, and Feng Xu

State Key Laboratory of Geomechanics and Geotechnical Engineering, Institute of Rock and Soil Mechanics, Chinese Academy of Sciences, Wuhan 430071, China

Correspondence should be addressed to Yintong Guo; ytguo@whrsm.ac.cn

Received 3 November 2017; Revised 17 January 2018; Accepted 28 January 2018; Published 20 March 2018

Academic Editor: Xiang Fan

We investigated the mechanical properties of mature bedding shale under cyclic loading conditions, with an application to the design of hydraulic fracturing in shale gas wells. Laboratory experiments were conducted on shale samples under two principal loading orientations. Testing results showed that accumulated fatigue damage occurs in a three-stage process. Analysis of fatigue damage at different maximum stress levels shows that fatigue life increases as a power-law function with maximum stress decreasing. And the maximum stress significantly affects the fatigue life. Further, the elastic part of shale rock deformation was recovered in the unloading process, whereas the irreversible deformation remained. The irreversible deformation, growth trend, and accumulation of the total fatigue were directly related to the fatigue damage. This process can be divided into 3 stages: an initial damage stage, a constant velocity damage stage, and an accelerated damage stage, which accounted for about one-third of the fatigue damage. Shale rock is a nonhomogeneous material, and the bedding is well developed. Its fatigue life differs greatly in two principal loading orientations, even under the same loading conditions. All of these drawn conclusions are of great importance for design of hydraulic fracturing in shale gas wells.

1. Introduction

In recent years, with the development of unconventional oil and gas resources, hydraulic fracturing technology has been paid more attention. To ensure the success of hydraulic fracturing, it is necessary to understand the mechanical properties of shale formations. In such processes, a network of cracks is obtained through both artificial fracture and natural cracks in the formation. Under different sedimentary environment conditions, the bedding density of shale formation has a great difference. Therefore, the bedding plays a significant role in both mechanical behavior and engineering activities [1]. During long horizontal-section drilling and hydraulic fracturing construction engineering, the surrounding rock is subjected to loading and unloading states. The mechanical properties of shale under dynamic loads differ dramatically from those under static loads. However, the nature of dynamic failure in the rock remains unclear, especially under cyclic loading conditions. Therefore, it is of great significance to study the mechanical behavior of shale rock under cyclic loading.

The long-term stability of rock mass depends on rock fatigue failure mechanisms. Although the deformation characteristics and failure mechanism under cyclic loading are related to the static load, there is a significant difference between the two cases.

During the last few decades, a lot of research has focused on the response of rocks under cyclic loading. The fatigue properties of rock materials have been found to be dependent on variables such as the amplitude, the upper limit stress, and frequency [2–4]. It has also been reported that different materials show different responses when they are subjected to cyclic loading—some materials become stronger and more ductile, while others become weaker and more brittle [2].

Previous studies [5, 6] show that the fatigue damage of rock has a "threshold value," when the maximum stress value is lower than a certain value, the sample cannot be

Table 1: The mineral compositions of shale rocks.

	Montmorillonite	Illite	Quartz	Cristobalite	Albite	Calcite	Muscovite	Pyrite	Annite	Ankerite
Shale	1.66	3.60	50.23	4.75	17.60	2.60	5.71	5.80	3.83	4.21

destroyed no matter how many load cycles are applied; thus, the maximum stress has an important influence on the fatigue life. The mechanical properties of rock samples under monotonic and cyclic loadings were also studied [7], it was found that under monotonic loading, thenardite and glauberite samples show an elastic-plastic style; however, under cyclic loading, it changed to a ductile style. There have also been several studies on the fatigue properties of rock salt subjected to interval cyclic pressures [2, 8, 9]. In one of these studies, an empirical model fitting the relationship between fatigue life and interval cyclic pressure was established. In another, a series of laboratory tests were performed to assess the effects of cyclic loading on compressive strength, elasticity, and time-dependency of Maha Sarakham rock salt, the results indicate that the salt compressive strength decreased with increasing number of loading cycles and was best represented using a power-law equation [8].

From the above study, it is evident that fatigue tests have been carried out for the most common types of rocks in geotechnical engineering. However, the main rocks involved are sandstone, marble, granite, salt rock, and so on. The rock types are fairly homogeneous, and almost no stratified sedimentary rocks are involved. There is a great difference on deformation mechanism between the homogeneous rock and the layered rock. The angle between the loading direction and the bedding has an important influence on the mechanical properties and failure modes for layered rock.

During hydraulic fracturing processes in shale gas reservoirs, the changing of drilling mud density causes stress fluctuations in the surrounding rock during long horizontal well drilling. In the hydraulic fracturing stage, pressure fluctuations in hydraulic fracturing fluid can be clearly observed, with more than twenty circulates commonly obtained. The shale rock mass is subjected to repeated loading and unloading cycles; therefore, accurate assessment of the shale reservoir crushing effect and long-term stability of the well-bore during hydraulic fracturing is an important practical significance.

There are many sets of small layer shale formation with different mechanical properties and bedding densities in Jiao Shiba, China. Understanding the fracture characteristics of shale rock under cyclic loading is of great practical significance to accurately evaluate the fracturing effects and long-term stability of shale reservoirs. The objective of this research is to experimentally determine the effects of cyclic loading on mature bedding shale under two principal loading orientations. Using RMT-150C rock mechanics test system, the axial deformation, strength characteristics, and rupture mode of the cycle loading were studied and analyzed, and some useful conclusions were obtained which could provide effective technical parameters for hydraulic fracturing.

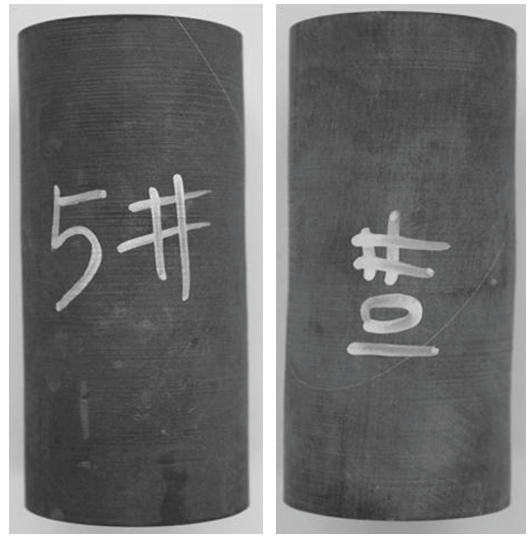

Figure 1: Typical shale samples before testing.

2. Experimental Approach

2.1. Specimens. The shale samples used in the experiment were collected from Longmaxi formation at Nanchuan outcrop in Chongqing Province, China. In this paper, the shale samples adopted with well-developed bedding; in one meter, the number of bedding is more than 200. The main components of specimens were quartz, clay minerals, and feldspar, with a small amount of muscovite. The mineral compositions are shown in Table 1.

The fatigue properties of shale rock were studied under cyclic loading with two principal loading orientations: parallel and perpendicular to the bedding planes, respectively. Shale samples with similar P-wave velocities were selected for cyclic loading tests. ISRM standards [10] were followed when cutting the samples into standard cylinders with a diameter-to-length ratio of 1 : 2, specimen's diameter is 50 mm, and its height is 100 mm. The degree of parallelism between the upper and lower ends is within 0.03 mm; typical shale samples before testing are shown in Figure 1. Three shale samples for each coring direction were carried out on uniaxial compression tests to ensure that the results were representative, and the residual samples were used for cyclic loading tests. The average density was 2.665 g/cm^3, and the average porosity was 1.25% by the mercury intrusion method. The average P-wave velocity of vertical coring samples (numbered H) was 4667 m/s, and the average P-wave velocity of parallel coring samples (numbered V) was 4306 m/s. Horizontal permeability mainly ranged between 0.0338 and 0.0581 mD, with an average value of 0.04595 mD, and vertical permeability was lower than horizontal permeability, with a difference of more than 2 orders of magnitude. The shale samples also show obvious anisotropic characteristics.

Table 2: Mechanical properties of shale samples under uniaxial compression test.

Sample number	Axial stress (MPa)	Elastic modulus (GPa)	Poisson ratio
H-11	87.27	14.66	0.321
H-12	84.25	16.69	0.337
H-13	87.09	16.49	0.290
Average	86.20	15.95	0.32
V-11	119.25	15.10	0.282
V-12	112.81	15.41	0.281
V-13	117.42	15.27	0.262
Average	116.49	15.26	0.275

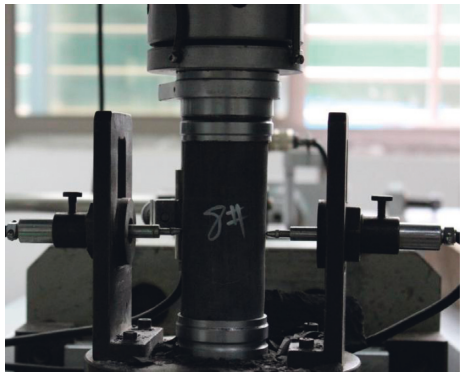

Figure 2: Apparatus and schematic.

2.2. Experimental Design. Prior to carrying out cyclic loading tests, the mechanical properties of shale samples under uniaxial compression tests were measured, as shown in Table 2.

The mechanical properties of shale are obtained by uniaxial compression test, which provides a reference for the upper limit stress setting of cyclic loading test. Uniaxial compression tests were performed on three samples each of vertical and parallel coring, respectively. All the tests were performed using a RMT-150C electrohydraulic servo-control testing machine, as shown in Figure 2. Displacement control mode with a loading rate of 0.003 mm/s was used for uniaxial compression tests, and loading control mode was used for cyclic loading tests. For cyclic loading tests, the axial loading was specified as a sinusoidal cyclic compressive load, and the loading frequency was set to 0.5 Hz. The cyclic tests were conducted at four different maximum stress amplitudes on the parallel and vertical coring samples. The maximum stress level (the ratio of maximum cyclic stress to the average of uniaxial compression strength) was varied from 0.95 to 0.80. Initially, the sample was loaded up to the mean-stress level in the displacement control mode, and then the cyclic test was performed at a given amplitude and frequency. It should be noted that the predetermined stress amplitude for the machine was equal to one-half of the total range [11].

Finally, the results of the fatigue tests were analyzed in relation to various parameters such as axial strain, cycle times, and rupture mode. The fatigue test characteristics are shown in Table 3.

3. Test Results and Analysis

3.1. Uniaxial Compressive Strength and Deformation. Table 2 shows the results under uniaxial compression tests. The stress-strain curves are shown in Figures 3 and 4. The stress shows a maximum value with increasing axial strain before decreasing rapidly. The samples show obvious brittleness characteristics. For two principal loading orientations, the compressive strength and elastic modulus were obviously anisotropic, as there were great differences. For parallel coring samples, the average peak stress is 86.20 MPa, and average elastic modulus is 15.95 GPa. In these samples, split tensile failure occurred, with the specimen being split into multiple independent pieces almost parallel to the bedding surfaces. For vertical coring samples, the average peak stress is 116.49 MPa, and average elastic modulus is 15.26 GPa. The initiation of microcracking occurred along the bedding plane, and it gradually runs through the bedding plane and causes the specimen destruction, resulting in an approximately parallel layered block. Also, the reproducibility of these experiments was well, thus providing a basis for selection and comparison of the control indexes of the cycle test.

3.2. Comparison between Cyclic Loading and Uniaxial Compression. Under cyclic loading, the failure process of shale rock is different from that under static uniaxial compression; however, there is some relationship between the two cases [12]. The axial stress-strain curves under uniaxial compression and cyclic loading are drawn on the same diagram (for parallel coring samples) in Figure 5. The upper limit stress ratio of the cycle test was 0.90, and the amplitude stress ratio was 0.65; it shows that the end deformation is consistent with uniaxial loading failure deformation. The figure indicates that the failure occurs below the maximum strength loading condition, as a result of accumulative damage. There are two main stages of axial strain: stable crack propagation and unstable crack propagation, resulting in a sudden breakdown. Figure 6 shows the stress-strain curves for uniaxial compression (sample V-13) and cyclic loading (sample V-3) tests. The upper limit stress ratio of the cycle test was 0.95, and the amplitude stress ratio was 0.81. The end of the cyclic loading deformation was larger than uniaxial compression failure. In addition, the cumulative deformation in vertical bedding planes was relatively large. It is analyzed that, under uniaxial

Table 3: Summary of the fatigue test characteristics.

Sample number	The upper limit stress	The lower limit stress	Maximum stress level	Minimum stress level	Amplitude level	Frequency (Hz)	Number of failure cycles
H-1	81.75	16.4	0.95	0.19	0.76	0.5	11
H-5	77.58	21.75	0.9	0.25	0.65	0.5	155
H-6	73.27	28.1	0.85	0.33	0.52	0.5	1856
H-8	68.92	34.13	0.8	0.40	0.40	0.5	5689
V-1	110.64	16.2	0.95	0.14	0.81	0.5	27
V-3	104.85	29.12	0.9	0.25	0.65	0.5	452
V-4	99.02	38.44	0.85	0.33	0.52	0.5	2569
V-10	93.2	47.76	0.8	0.40	0.40	0.5	8956

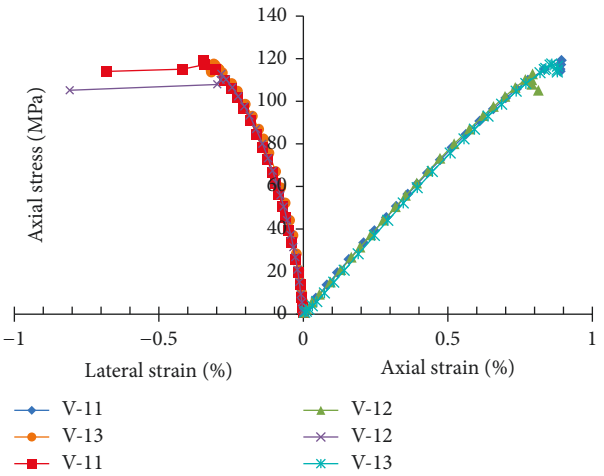

Figure 3: Stress-strain curves of shale under uniaxial compression test (vertical coring).

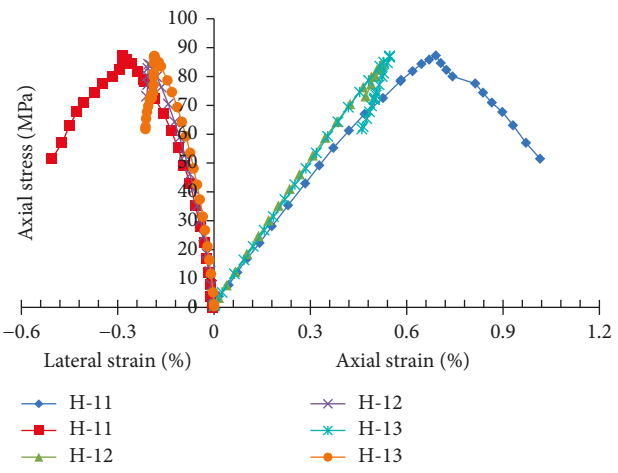

Figure 4: Stress-strain curves of shale under uniaxial compression test (parallel coring).

compression, the sample is always in the stage of increasing load, and partial failure of specimen causes the failure of the whole specimen. However, under cyclic loading and unloading conditions, the local stress state of the bedding plane can be adjusted, so the specimen is fully deformed during fatigue failure. The cyclic loading results showed that the fatigue failure consisted of three stages: an initial stage of fatigue fracture (initiation phase I), a stable crack propagation (uniform velocity phase II), and an unstable crack propagation, resulting in a sudden breakdown (accelerated phase III). These three steps have also been reported in previous studies [13, 14]. The fatigue process is related to accumulative damage, which oftentimes leads to a progressive weakness of materials. Variation of these parameters with time or cycle number can be observed in all three stages of fatigue damage.

3.3. The Effect of Maximum Stress. The relationship between maximum cyclic loading ratio and fatigue damage cycle number for two principal loading orientations is illustrated in Figure 7. The effect of maximum stress on fatigue life indicates that the relationship between the maximum stress and fatigue life is subordinate to the power-law function. For parallel coring samples, when the applied maximum stress level was 0.95, the sample damaged after 11 cycles. However, when the maximum stress level was 0.80, the failure stress obtained was from 81.75 MPa to 68.92 MPa, as the rock fatigue damage after 5689 cycles was 517 times that for specimen H-1. It is evident that the damage grew very slowly as the maximum stress ratio 0.80 was close to the fatigue threshold. For vertical coring samples, the failure stress obtained from 116.49 MPa to 93.2 MPa, with fatigue damage after 8956 cycles. With the same upper limit for the stress ratio, the fatigue life cycle for vertical coring was longer than that of parallel coring. Results were shown that the damage from cyclic loading on shale rock was weakened when the normal stress was perpendicular to the bedding plane.

The relationship between axial strain and relative cycle (ratio between cycle number and failure cycle number) at four different maximum stress levels 0.95, 0.90, 0.85, and 0.80 is illustrated in Figure 8. Figures 8(a) and 8(b) indicate that, at 0.95 maximum stress levels, during the fatigue life, the axial strain has no obvious turning point. However, for other upper limit stress conditions, the axial strain can be divided into 3 stages: an initial deformation stage, a constant velocity deformation stage, and an accelerated deformation stage, with the second stage being dominant.

The first stage, that is, the development of axial strain rate, is fast, as the sample accumulates a large deformation in a short time period; this leads to the second stage, when the strain rate is relatively stable and the axial strain development is very slow, resulting in a very long process, which occupies most of the fatigue life. In the third stage, the axial

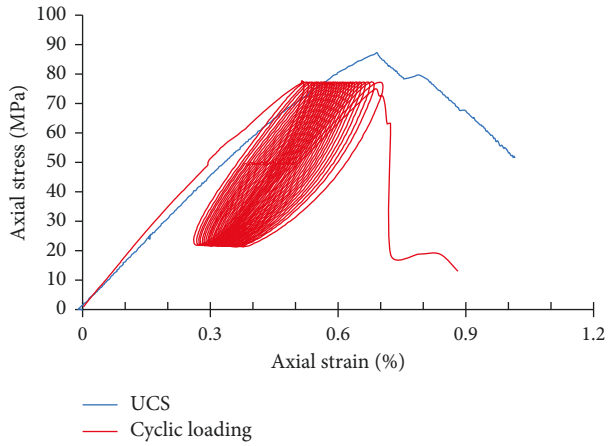

Figure 5: Stress-strain curves for uniaxial compression (sample H-12) and cyclic (sample H-2) loading tests.

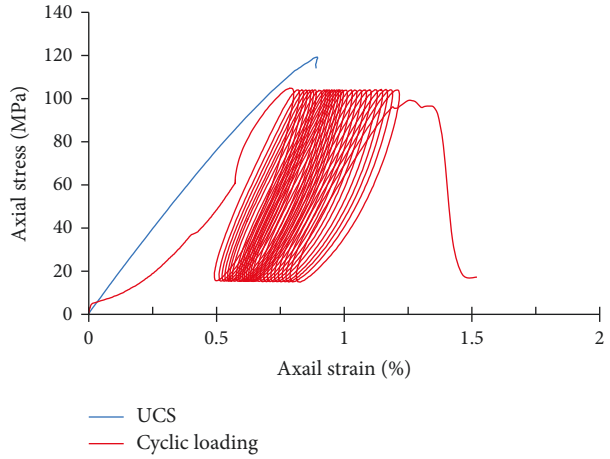

Figure 6: Stress-strain curves for uniaxial compression (sample V-13) and cyclic (sample V-3) loading tests.

strain rate increases rapidly, and the specimen is destroyed quickly. And this process takes a very short time, and the number of cycles are also few, as the accumulative effects of the three deformation stages lead to final failure. The curve in the initial deformation stage shows a larger initial axial strain, while the process of loading and unloading is accompanied by the slow accumulation of damage. With the increasing in axial loading, the internal pores and fissures are closed, the structure becomes denser, and the overall stiffness is improved.

Under cyclic loading, the elastic deformation will be recovered in the process of unloading, but the irreversible deformation will be remained. The irreversible deformation, growth trend, and accumulation of total fatigue are directly related to the fatigue damage. Hence, the study of irreversible deformation of fatigue failure is more scientific and precise.

Figure 9 shows the relationship between irreversible axial deformation and relative cycle (ratio between cycle number and failure cycle number). It can be seen that the fatigue process of irreversible deformation may be divided into 3

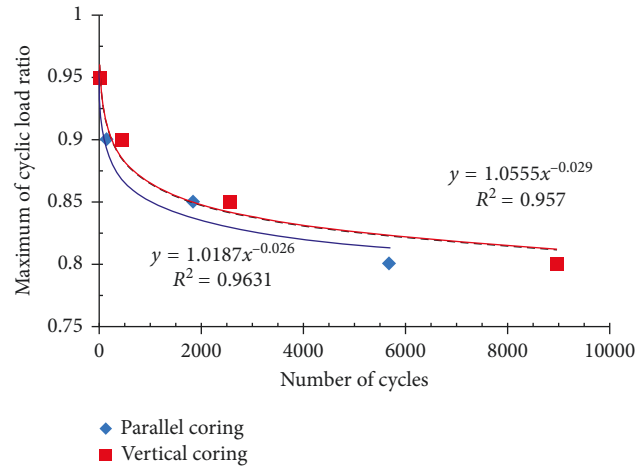

Figure 7: The relationship between maximum cyclic loading ratio and fatigue damage cycle number (frequency 0.5 Hz).

stages: an initial stage, when the development speed is fast; a second stage, after a certain period of time, the development speed gradually stabilizes, becoming constant; a third near-destruction stage, when the development speed gradually accelerates towards destruction. The irreversible deformation gradually accumulates with the continuous action of cyclic loading, until the specimen is destroyed. Therefore, the fatigue failure of shale rock is progressive accumulation of irreversible deformation in axial direction. For parallel coring samples, the irrecoverable deformation was relatively small at the initial stage of the cycle, and irreversible deformation was mainly produced in the third stage. For vertical coring samples, the irreversible deformation ratio was greater than that for parallel coring in the initial stage, and cumulative irreversible deformation was mainly completed in the first and second stages.

3.4. Fatigue Damage Evolution Characteristics. Under the action of the loading, the localized microcracks in the samples affected the strength of rock material before macrocracking had occurred. From the point of view of damage mechanics, Lemaitre, considering the failure process, proposed the concept of continuum damage mechanics [15].

Using the definition of damage variation [16], the data obtained in this study were used to calculate the relationship between damage variation and cyclic numbers, as shown in Figure 10. It indicates that according to the cyclic fatigue, the damage may be divided into 3 stages. In the initial stage, the damage variable increased with increasing the number of cycles, and this stage accounted for one-third of the total damage. The second stage occurred after a certain number of cycles, wherein the microcracks were closed as the new growth gradually stabilized, and the damage variable increased slowly. Once the damage accumulated to a certain extent, a lot of new cracks began to appear and gradually connected causing the damage variable to increase rapidly; that was the third stage. Fatigue failure occurred when a large number of cracks coalesced into a macrocrack. Out of these stages, the constant velocity occupied most of the

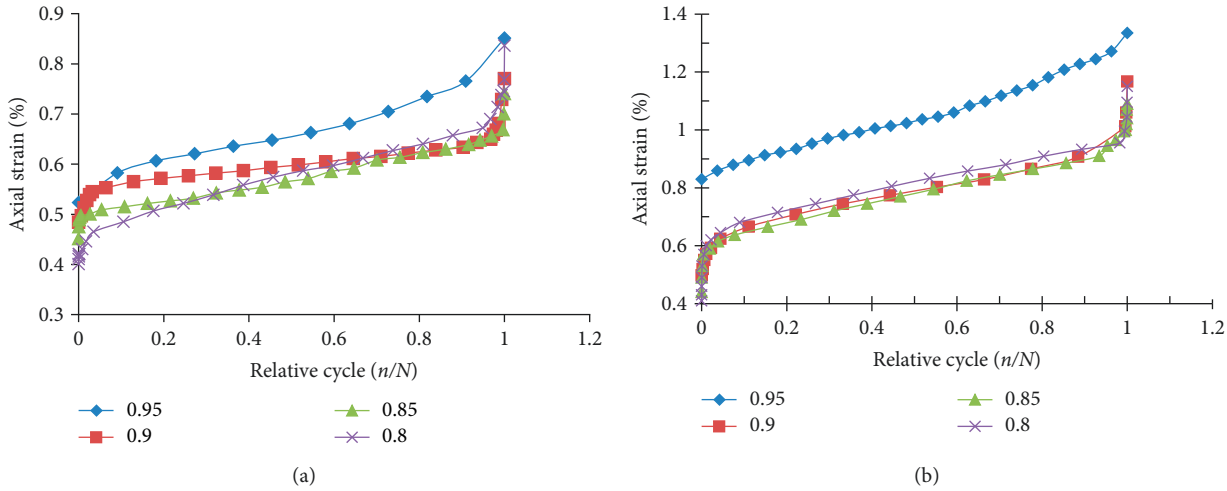

Figure 8: The relationship between axial strain and relative cycle. (a) Parallel coring; (b) vertical coring.

fatigue life, although the cumulative amount of deformation was only one-third of the total. The remaining two stages experienced a relatively short time, but the accumulation of deformation during these stages was very large.

At the same time, different coring angle specimens show different characteristics in Figures 10(a) and 10(b). For parallel coring samples, the first stage of the damage variable is about 0.3, and the slope of second stage is larger. The trend is similar under different maximum stress conditions. For vertical coring samples, when the applied maximum stress level was 0.95, there was no obvious third stage of the damage variable. It indicates that, at 0.95 loading stress levels, the damage variable and the number of cycles were directly proportional, and no obvious turning point was observed; therefore, damage was produced continuously with an increase in the number of cycles. Under other stress levels, the first stage of the damage variable is about 0.4, and the slope of second stage is smaller than parallel coring samples. These differences indicate that the initial damage is greater under condition of the loading direction perpendicular to the bedding surface.

The behavior of damage evolution is greatly dependent on the maximum stress, amplitude, and fatigue initial damage. The increase of these variables causes the second stage to be shortened, which is related to the whole fatigue process [17].

3.5. Deformation Modulus and the Number of Cycles. Figure 11 shows the relationship between the deformation modulus and relative cycle times. It can be seen that, under initial cyclic loading, the deformation modulus increased slightly with increasing cycle number. The relationship between deformation modulus and relative cycle times may be divided into 3 stages. In the first stage, the deformation modulus increased gradually with increasing cycle times, the change was mainly due to the closure of rock pores and microcracks. For vertical bedding coring samples, in initial cycle stage, the increase of deformation modulus is more than 6 GPa. The main reason is that the bedding plane is compacted. For parallel bedding coring samples, the increase of deformation modulus is smaller. It is mainly because the loading direction is parallel to the bedding plane, and the effect of compaction is limited. In the second stage, the deformation modulus is decreasing slowly during a long period, which occupies most of the cycle time. Different coring angle specimens show an approximate same trend. The third stage corresponds to the accelerated phase of fatigue deformation, after the sample has experienced several cycles. The deformation modulus reduced, and the specimen damaged. When the ratio of the upper limit stress is 0.95, the change in the deformation modulus was very evident.

3.6. Fatigue Fracture Characteristics. Figure 12 shows the typical failure modes after fatigue test. As seen in Figure 12 (a), it indicates that the failure mode of parallel coring samples was mainly tensile failure mode. The samples were decomposed into smaller parallel blocks, through the tensile failure of multiple layer surfaces, and the microcracks had enough time to start, spread, and coalesce under cyclic loading. The internal stresses were adjusted and redistributed with the crack initiation and propagation, and the whole fracture was divided into a number of slices. As seen in Figure 12(b), vertical coring specimens formed a number of cut bedding planes after cyclic loading. The failure mode was mainly mixed failure and dominated by tension cracks and shear cracks. The main part of the specimen fell as a powder on the test platform, with a very full rupture. In the process of hydraulic fracturing, if natural fractures and microfractures are present, the fracture pressure required to extend the cracks will be lower; thus, it is easier to form a fracture network.

4. Discussion

Hydraulic fracturing technology is the key technology for developing shale reservoir.

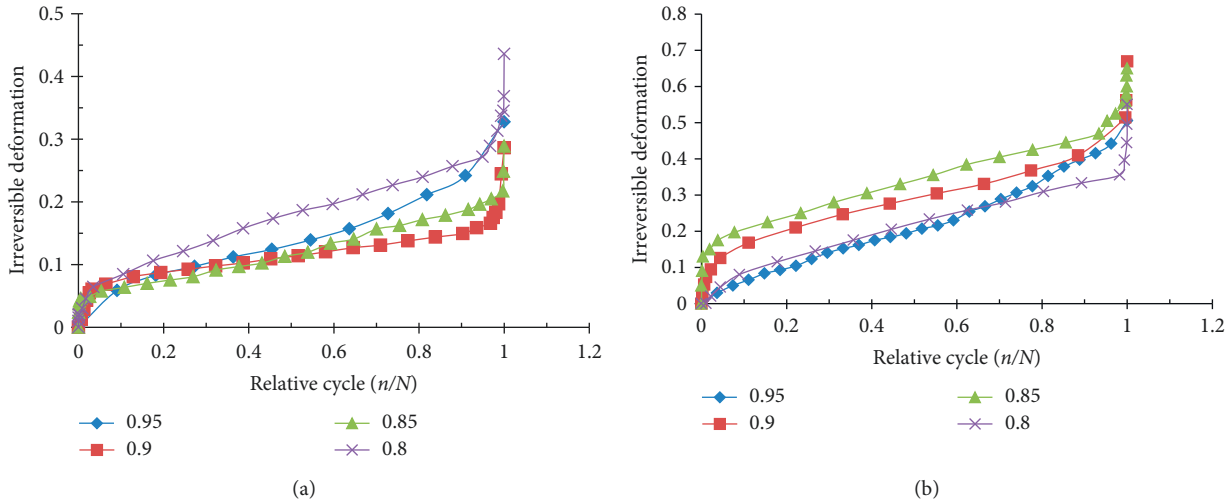

Figure 9: The relationship between irreversible deformation and the number of cycles. (a) Parallel coring; (b) vertical coring.

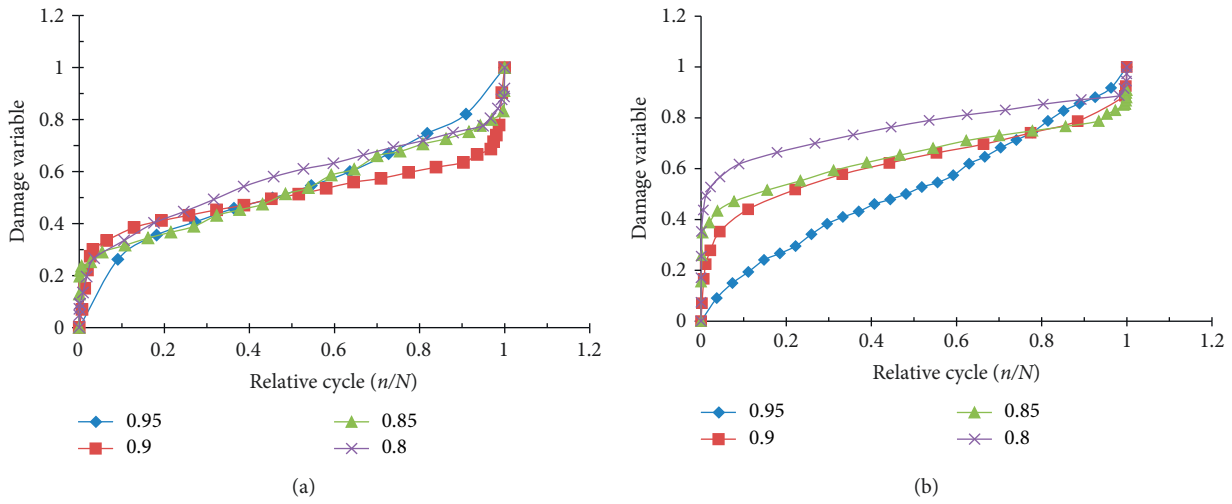

Figure 10: Damage variable versus cyclic numbers. (a) Parallel coring; (b) vertical coring.

In hydraulic fracturing engineering, the focus is on the strength and fracture characteristics of shale, which often refer to the value under static loading. However, pressure fluctuations in hydraulic fracturing fluid can be clearly observed, with more than twenty circulates obtained. Hence, the stress-level- and stress-path-dependent deformation and strength property of shale rock, which dramatically differs from that under monotonic or static load, are of great importance to long-term stability of the well-bore and form complex fracture network. A large number of testing results demonstrate that the peak strength of rocks decreases by 65% due to crack growth when cyclic loading is considered [7]. Testing results in this paper demonstrate that, under cyclic loading, shale rocks fail at a stress close to 80% of the peak strength under monotonic loading. Fatigue life increases in a power function with decreasing the maximum stress for the two cases. In addition to increases in fatigue life, the steady stage slope decreases. Also the angle between loading direction and bedding plane directly affects the characteristics of fatigue test. For parallel coring samples, the end deformation of fatigue test is consistent with uniaxial loading failure deformation. But the rupture mode is more broken than uniaxial compression. This indicates that, in the process of hydraulic fracturing, the fluctuation of water pressure helps to open more bedding surfaces, to form complex network crack. For vertical coring samples, the specimen is very fully damaged after the fatigue load. Analysis of fatigue damage variable at different load levels shows that when the maximum load level is decreased, the process of crack initiation occupies a large proportion of the whole fatigue life, while crack growth occurs at higher stresses. When hydraulic fracturing is carried out in the reservoir of bedding shale reservoir, the original natural lamination seam can be activated by adjusting the pressure of hydraulic fracturing pump.

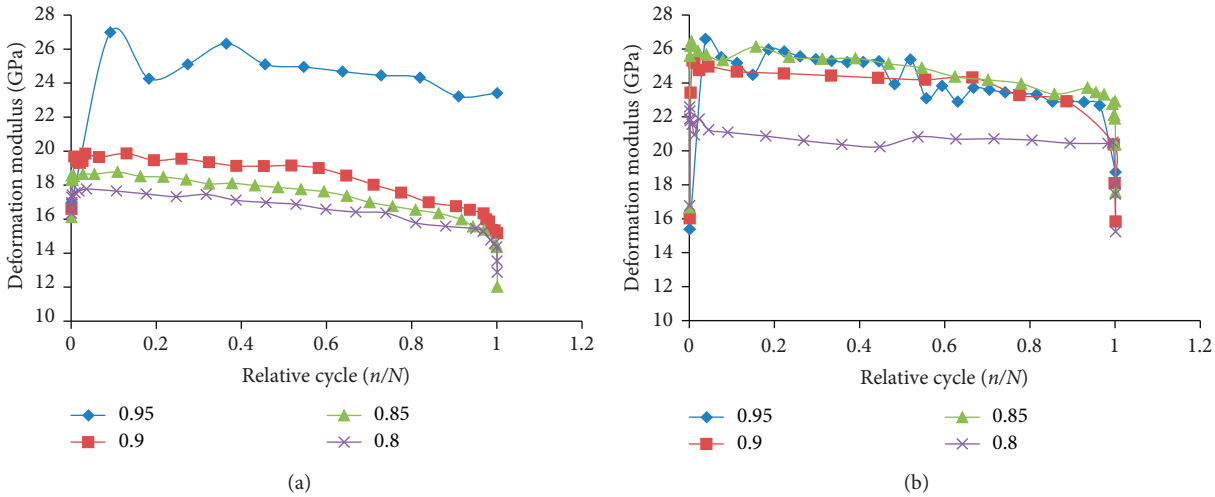

Figure 11: The relationship between fatigue deformation modulus and relative cycle times. (a) Parallel coring; (b) vertical coring.

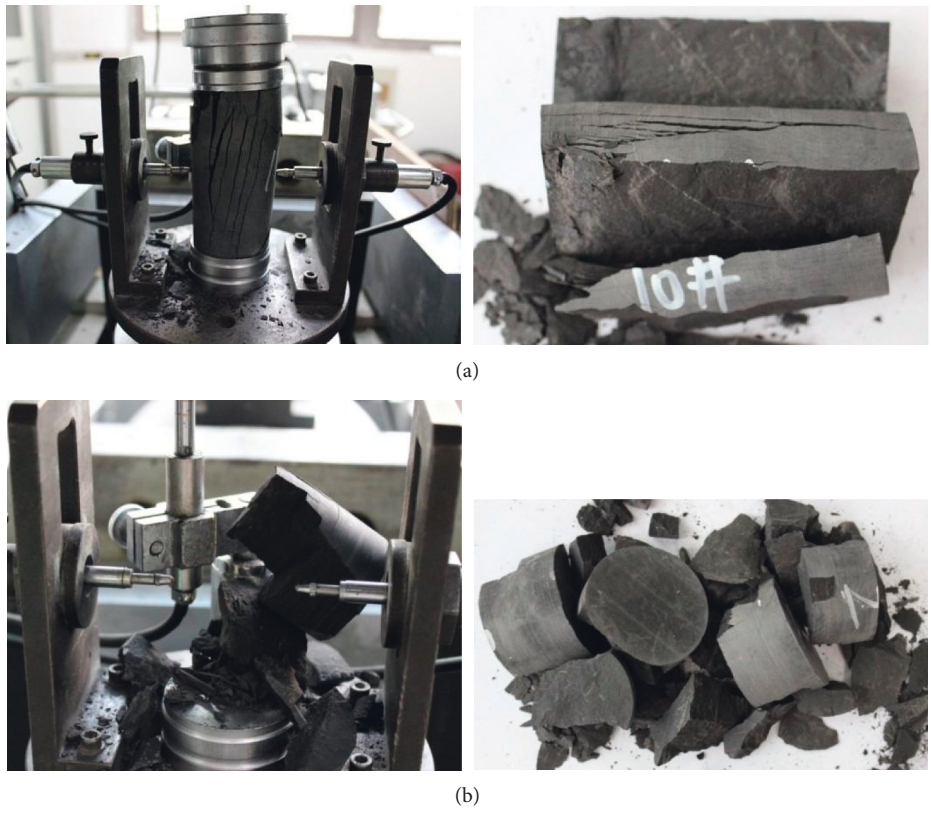

Figure 12: Typical failure modes after fatigue test. (a) Parallel coring; (b) vertical coring.

5. Conclusions

In order to understand the fatigue behavior of shale rock, samples were subjected to uniaxial cyclic loading in two principal loading orientations, for different maximum stress levels and amplitudes. Two failure modes were discovered through the analysis of the fracture morphology, the stress-strain curves under uniaxial compressive and cyclic loading, the effect of maximum stress, and the characteristics of fatigue damage evolution. The results show that the cyclic loading effect is clear. In summary, several conclusions can be made:

(1) Accumulated fatigue damage occurred in a three-stage process. At different maximum stress level, the fatigue life increases as a power-law function with decreasing maximum stress, and changing the maximum stress significantly affected the fatigue

process; the process of crack initiation occupies a large proportion of the whole fatigue life, while crack growth occurs at higher stresses. At the same time, different coring angle specimens show different characteristics, for vertical coring samples, the initial damage is greater under condition of the loading direction perpendicular to the bedding surface.

(2) Experimental results demonstrate that, after a few initial cycles, the shale rocks exhibited almost elastic behavior, and the elastic deformation was recovered in the process of unloading, but the irreversible deformation remained. With the increasing number of cycles, the irreversible deformation is observed. The maximum stress directly affects the axial strain value of ultimate failure.

(3) Shale rock is a nonhomogeneous material, and its fatigue life differs greatly in two principal loading orientations, which results in great difficulty in conducting fatigue analysis. The fatigue damage process may be divided into 3 stages: an initial damage stage, a constant velocity damage stage, and an accelerated damage stage which accounted for about one-third of the total damage. In order to effectively activate the original bedding plane or natural cracks, first of all, the distribution mode of natural cracks and bedding plane should be mastered; then, the number of cycle times and the maximum of the pump pressure can be adjusted as far as possible.

Conflicts of Interest

The authors declare that there are no conflicts of interest regarding the publication of this paper.

Acknowledgments

The research was supported by the National Natural Science Foundation of China (51574218), National Science and Technology Major Project of China (2016ZX05060-004 and 2017ZX05036-003), and Research on Key Scientific and Technical Issues in Exploration and Development of Shale Gas (XDB10040200), CAS Pilot Project (B). The authors would like to express our greatest gratitude for their generous support.

References

[1] J. Wang, L. Z. Xie, H. P. Xie et al., "Effect of layer orientation on acoustic emission characteristics of anisotropic shale in Brazilian tests," *Journal of Natural Gas Science and Engineering*, vol. 36, pp. 1–10, 2016.

[2] M. N. Bagde and V. Petros, "Waveform effect on fatigue properties of intact sandstone in uniaxial cyclical loading," *Rock Mechanics and Rock Engineering*, vol. 38, no. 3, pp. 169–196, 2005.

[3] J. Q. Xiao, D. X. Ding, G. Xu, and F. Jiang, "Waveform effect on quasi-dynamic loading condition and the mechanical properties of brittle materials," *International Journal of Rock Mechanics and Mining Sciences*, vol. 45, no. 4, pp. 621–626, 2008.

[4] M. N. Bagde and V. Petros, "Fatigue and dynamic energy behaviour of rock subjected to cyclical loading," *International Journal of Rock Mechanics and Mining Sciences*, vol. 46, no. 1, pp. 200–209, 2009.

[5] X. R. GE and Y. F. Lu, "Discussion about coal's fatigue failure and irreversible problem under cyclic loads," *Chinese Journal of Engineering*, vol. 14, no. 3, pp. 56–60, 1992.

[6] C. L. Feng, X. Q. Wu, D. X. Ding et al., "Investigation on fatigue characteristics of white sandstone under cyclic loading," *Chinese Journal of Rock Mechanics and Engineering*, vol. 28, no. 1, pp. 2749–2754, 2009.

[7] W. G. Liang, C. D. Zhang, and H. B. Gao, "Experiments on mechanical properties of salt rocks under cyclic loading," *International Journal of Rock Mechanics and Mining Sciences*, vol. 4, no. 1, pp. 54–61, 2012.

[8] F. Kittitep and P. Decho, "Effects of cyclic loading on mechanical properties of Maha Sarakham salt," *Engineering Geology*, vol. 112, no. 1–4, pp. 43–52, 2010.

[9] J. Y. Fan, J. Chen, and D. Y. Jiang, "Fatigue properties of rock salt subjected to interval cyclic pressure," *International Journal of Fatigue*, vol. 90, pp. 109–115, 2016.

[10] ISRM, "The complete ISRM suggested methods for rock characterization, testing and monitoring: 1974–2006," in *Suggested Methods Prepared by the Commission on Testing Methods*, H. Ulusay, Ed., International Society for Rock Mechanics (ISRM) Turkish National Group, Ankara, Turkey, 2007.

[11] A. Momeni, M. Karakus, G. R. Khanlari, and M. Heidari, "Effects of cyclic loading on the mechanical properties of a granite," *International Journal of Rock Mechanics and Mining Sciences*, vol. 77, pp. 89–96, 2015.

[12] Q. X. Zang, X. R. Ge, M. Huang et al., "Testing study on fatigue deformation law of red-sandstone under triaxial compression with cyclic loading," *Chinese Journal of Rock Mechanics and Engineering*, vol. 25, no. 3, pp. 473–478, 2006.

[13] J. Q. Xiao, D. X. Ding, G. Xu, and F. L. Jiang, "Inverted S-shaped model for nonlinear fatigue damage of rock," *International Journal of Rock Mechanics and Mining Sciences*, vol. 46, no. 3, pp. 643–648, 2009.

[14] E. Liu and S. He, "Effects of cyclic dynamic loading on the mechanical properties of intact rock samples under confining pressure conditions," *Engineering Geology*, vol. 125, pp. 81–91, 2012.

[15] Y. J. Yang, Y. Song, and J. Chu, "Experimental study on characteristics of strength and deformation of coal under cyclic loading," *Chinese Journal of Rock Mechanics and Engineering*, vol. 26, no. 1, pp. 201–205, 2007.

[16] Y. T. Guo, C. H. Yang, and H. J. Mao, "Mechanical properties of Jintan mine rock salt under complex stress paths," *International Journal of Rock Mechanics and Mining Sciences*, vol. 56, pp. 54–61, 2012.

[17] J. Q. Xiao, D. X. Ding, and F. L. Jiang, "Fatigue damage variable and evolution of rock subjected to cyclic loading," *International Journal of Rock Mechanics and Mining Sciences*, vol. 47, no. 3, pp. 461–468, 2010.